

LOGAN JOURNAL OF MULTIDISCIPLINARY EARTH SCIENCES, AND SUSTAINABILITY

ISSN: 3067-4395

LJMESS, 2023 11(3)

GRAVITY-BASED FAULT LINEAMENT MAPPING IN OLKARIA FIELD, KENYA

James Ndungu Wainaina

Geomatics Department, Jomo Kenyatta University of Agriculture and Technology, Kenya DOI: https://doi.org/10.5281/zenodo.17078089

Abstract: Geological faults are essential requirements in geothermal system. Lineament is an important feature in showing subsurface structures as faults. In recent years automatic lineament extraction has gained huge popularity as it circumvents issues such as errors and time constraints that associated with manual extraction procedure. This study aims to identify subsurface lineaments automatically from gravity data. Gravity data from Olkaria geothermal field was measured, corrected and a Bouguer anomaly obtained. Polynomial regression and Quadratic Square trend surface analysis techniques were used to filter the data into regional and residual anomalies. Subsurface lineaments were generated from the residual contour map using Gaussian filter edge detection and curve extraction parameters of the line module of the PCI Geomatica. Density lineaments map was extracted which displayed faulting of the area. Orientation of lineaments was presented using rose diagrams where the main trend of the subsurface fault structures was observed to be dominantly in NW-SE and the predominantly in N-S. Area with high density lineaments were located around the center of the field, while the west area of the field had less fracturing.

Keywords: Gravity, Lineaments, Geothermal

I. Introduction

Demands towards renewable energy has increased, geothermal energy gives a substantial contribution. Efficiency is therefore required to develop cites and increase efficiency of the existing systems. Geoscience plays a main role in optimizing and characterizing geothermal cites (Geowissenschaften, 2015).

Geothermal potential is enhanced by interconnection of fractures and faults network as this creates percolation threshold which allows sustainability of hydrothermal fluid flux. To obtain information regarding the permeable zone and indication of the reservoir zone for geothermal prospecting a geophysical method is required. One of the oldest and most widely used geophysical methods in exploration is the gravity method (Darmawan et al., 2021).

Lineament is a mappable rectilinear or curvilinear linear feature of a surface distinct from adjacent patterns and express an underlying geological structure, that is mappable (Nugraha et al., 2021). Gravity datasets can detect

lineaments through application of Gaussian kernel and gradient operator which are techniques used in an automated linear extraction where the image is automatically processed by specifying different parameters, such as the curve length, the connection of distance and kernel size. LINE module from PCI Geomatica has been the most popular processing tool in recent years in lineament extraction (Nugraha et al., 2021).

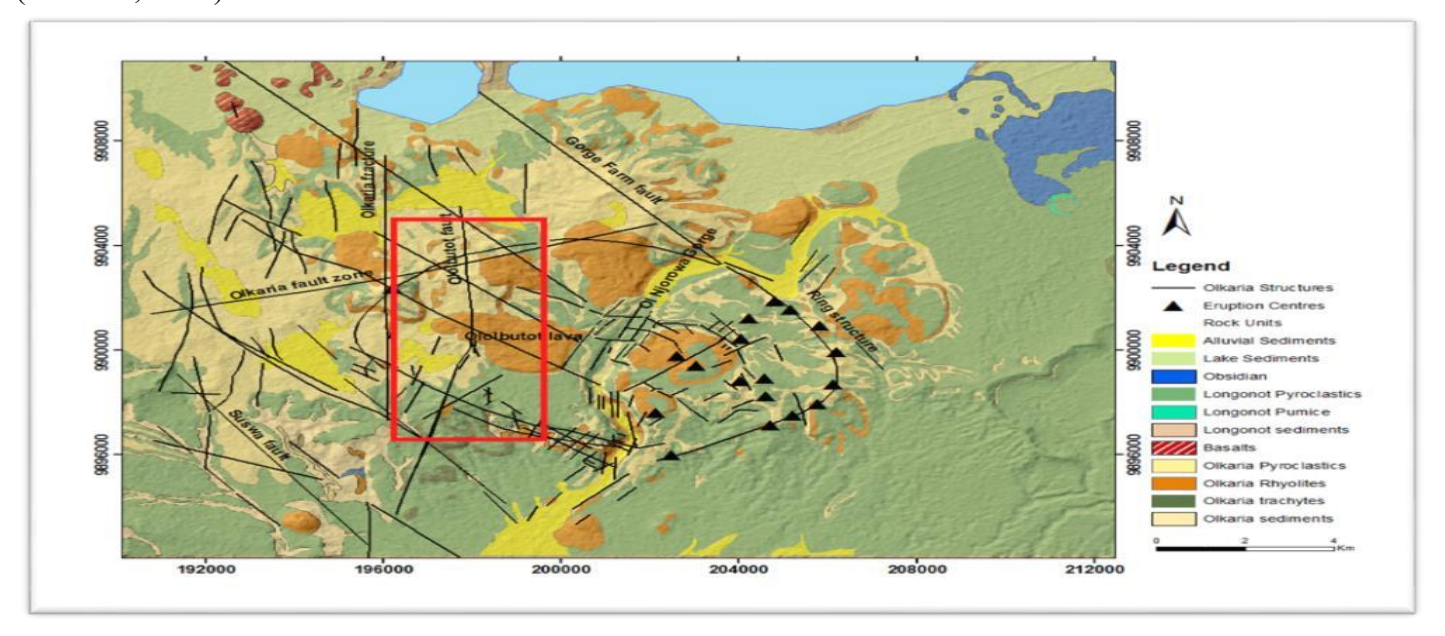
This study aims to identify sub-surface lineaments in the Olkaria geothermal field with gravity data using automatic lineaments. Main contribution is to show detailed structural analysis which help us understand the fluid flow in the Olkaria geothermal reservoir. This is essential for cite selection and smart drilling strategies which supports a sustainable exploration and helps avoid risks as low productive wells or high corroding waters (Geowissenschaften, 2015).

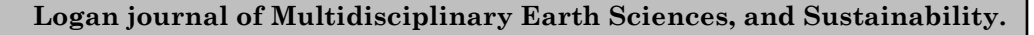
Geophysical studies have not given a good representation of the subsurface structure in this area. The data spread was also sparse and therefore could not demarcate the boundaries of the resource area (Ouma, 2007). NE-SW trending faults have low Chlorine content. The NW-SE trending faults bring in high temperature and Chlorine rich waters. The NE-SW trending Olkaria fracture tends to carry cool temperature waters that have led to a decline in enthalpies of the wells it cuts through (Wamalwa et al., 2016).

There is no explanation yet as to the existence of different reservoir characteristics in terms of structural settings. There could be major faulting separating the Olkaria aquifers for there to have different reservoir characteristics between the West and the East field (Geowissenschaften, 2015).

Geology of study area

Olkaria is a high-temperature geothermal system located within the central sector of the Kenya Rift Valley and associated with an area of late Quaternary rhyolitic volcanism (Fig.1). The geology is dominated by Pleistocene-Holocene, Holocene comenditic rhyolite flows on the surface and basalts, trachytes, and tuffs in the subsurface. The Olkaria field can be separated into east and west stratigraphic zones with the divide through the Olkaria Hill. The reservoir characteristics also follow this zonation. The geothermal reservoir in the east is hosted within Pleistocene Plateau Trachytes, while in the west it is within the Pliocene Mau Tuffs. Structural, geochemical, and hydrothermal alteration patterns indicate that the west field is at the margin of the larger Olkaria system. The anomalous bicarbonate enrichment in the west sector is due to additional adsorbed carbon dioxide from the mantle (Omenda, 1998).





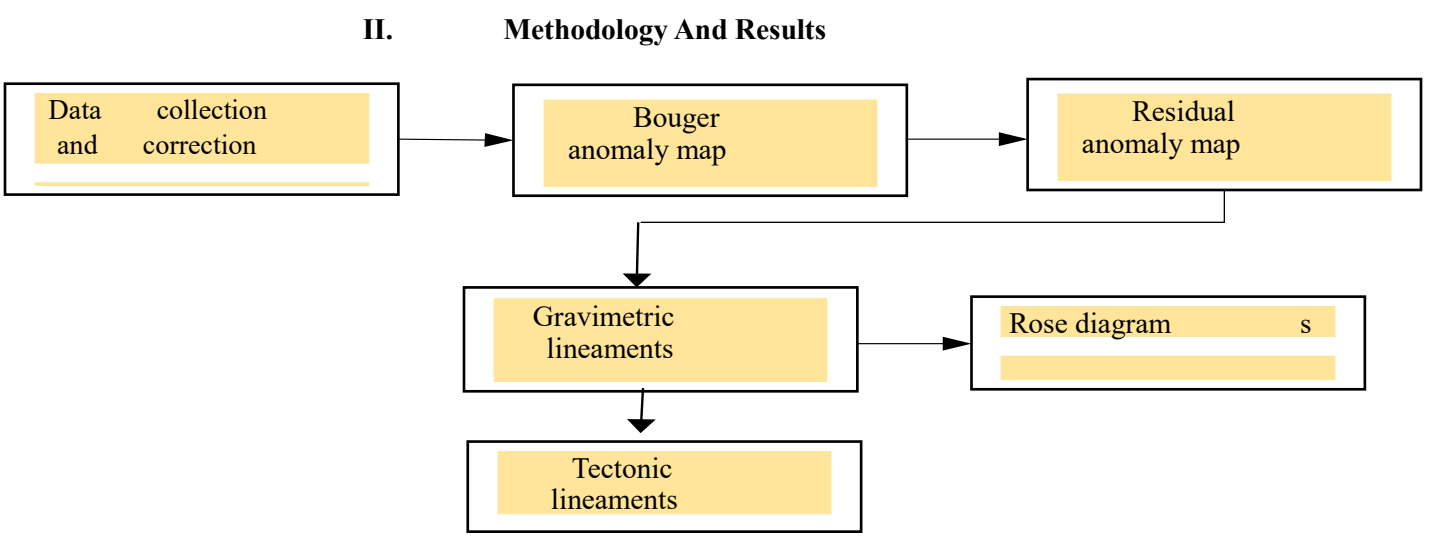


Fig. 1: Surface geology and structures in the Greater Olkaria geothermal area (Mariita et al., 2016) Workflow chart

This research was conducted in the Olkaria geothermal field with the geographical location coordinates 0° 49' 53.064" S, -36° -16' -39.943" W and 0° 55' 18.666" S, -36° -22' -35.239" W. A Scintrex CG-5 gravity meter with an accuracy of ± 0.001 mGal was used to take readings of 320 stations across the field. Bouguer gravity anomaly ΔgB was obtained from applying all the corrections as in Equation 1 below;

$$\Delta \mathbf{g} \mathbf{B} = \mathbf{g} m + (\Delta \mathbf{g} \mathbf{F} \mathbf{A} - \Delta \mathbf{g} B P + \Delta \mathbf{g} T + \Delta \mathbf{g} t i d e) - \mathbf{g} n$$

Where Δg_{BP} - Bouguer plate correction; Δg_{FA} - Free air correction; Δg_T - Latitude correction and $\Delta gt \ i \ de$ -Tidal correction, gm is the measured value and gn_n normal gravity value. The data was reduced with an average crustal density of $2.67 \mathrm{g/cm}^3$

Bouguer anomaly map with a contour interval of 5 gu was created as displayed in Fig. 2. Kriging gridding method was used in establishing of Bouguer anomaly contours. The Bouguer anomaly map shows local variations in the gravity field moving from -1775 gu to -1850 gu which are clearly displayed as an increasing regional gradient from North-West, North and North East region towards South-West, South and South-East region of the geothermal area.

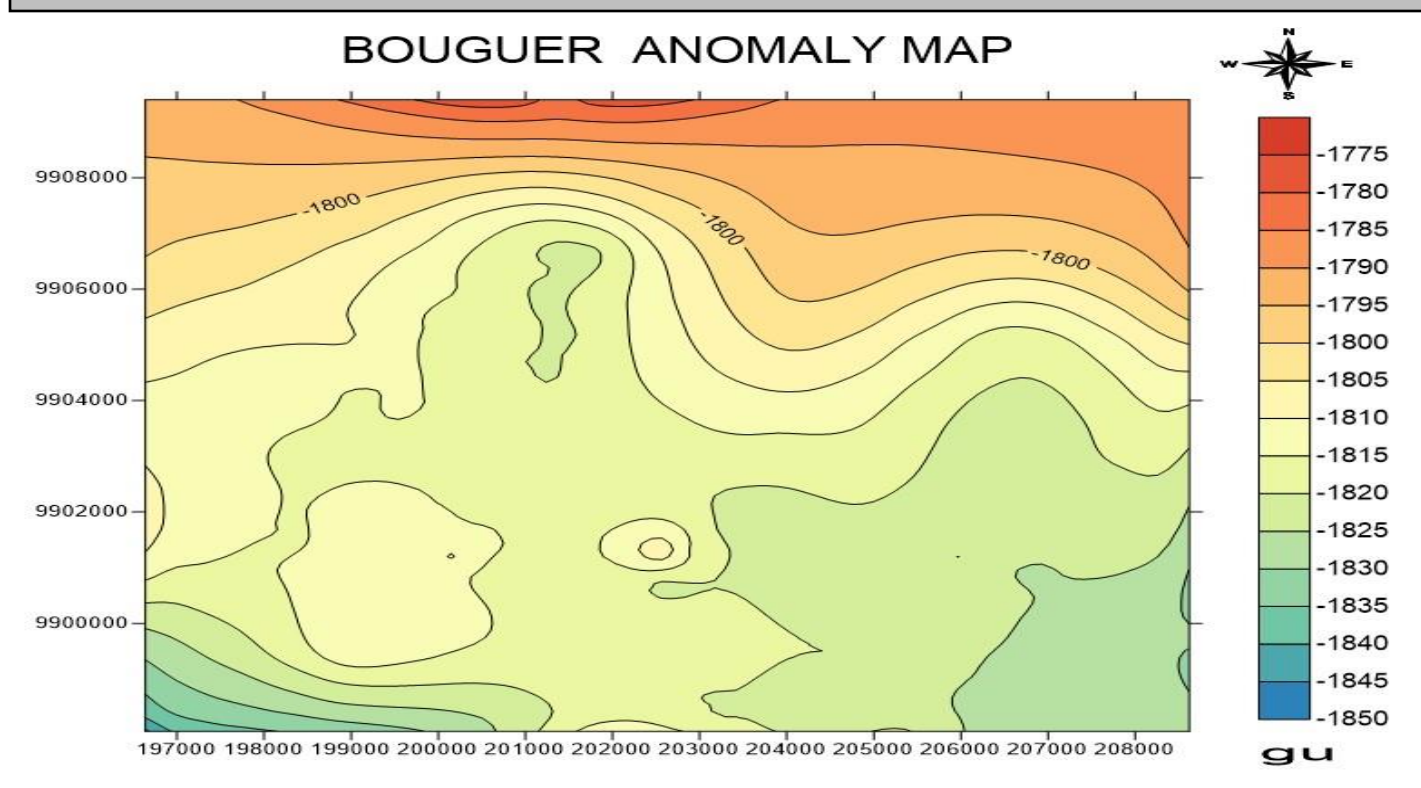


Fig. 2: Bouguer anomaly map (contour interval = 5 gu)

Separation of residual anomaly

The regional anomaly Fig. 3 assimilated to a plane, was estimated by using the polynomial regression gridding method and subtracted from the Bouguer anomaly in order to calculate the residual anomaly

Fig. using the Surfer software. SVD (Second Vertical Derivative) was used as a tool for delineation of anomalies due to its effectiveness in enhancing gravity data. It enhances subtle features of gravity data of particular interest that are not noticeable from the original data. In this case it was used in upward continuation to create the residual map. High gradients are associated with high contrast of physical properties of the subsurface (Darmawan et al., 2021).

Gradients, and also their magnitude, are usually employed to delineate boundaries of anomalous sources. The SVD of the vertical component of gravity, g_z , was used for calculations in the spatial domain from the horizontal gradients by using the Laplace's equation as the gravitational field obeys the Equation 2. The right hand of the equation represents the curvature in two mutually dependent horizontal directions and the negative sign indicates presence of a local maxima in the anomaly finding the second derivative, the linear component has been removed, retaining the sinusoidal component of short wavelength (Sumintadireja et al., 2018). The range of residual gravity value is about 26gu to -14gu as displayed in Fig. 4.

$$\frac{\partial^2 g_z}{\partial z} = -(\partial x^2 + \partial y^2)$$
 Equation 2
$$\frac{\partial^2 g_z}{\partial z} = \frac{\partial^2 g_z}{\partial z}$$

31 | Page

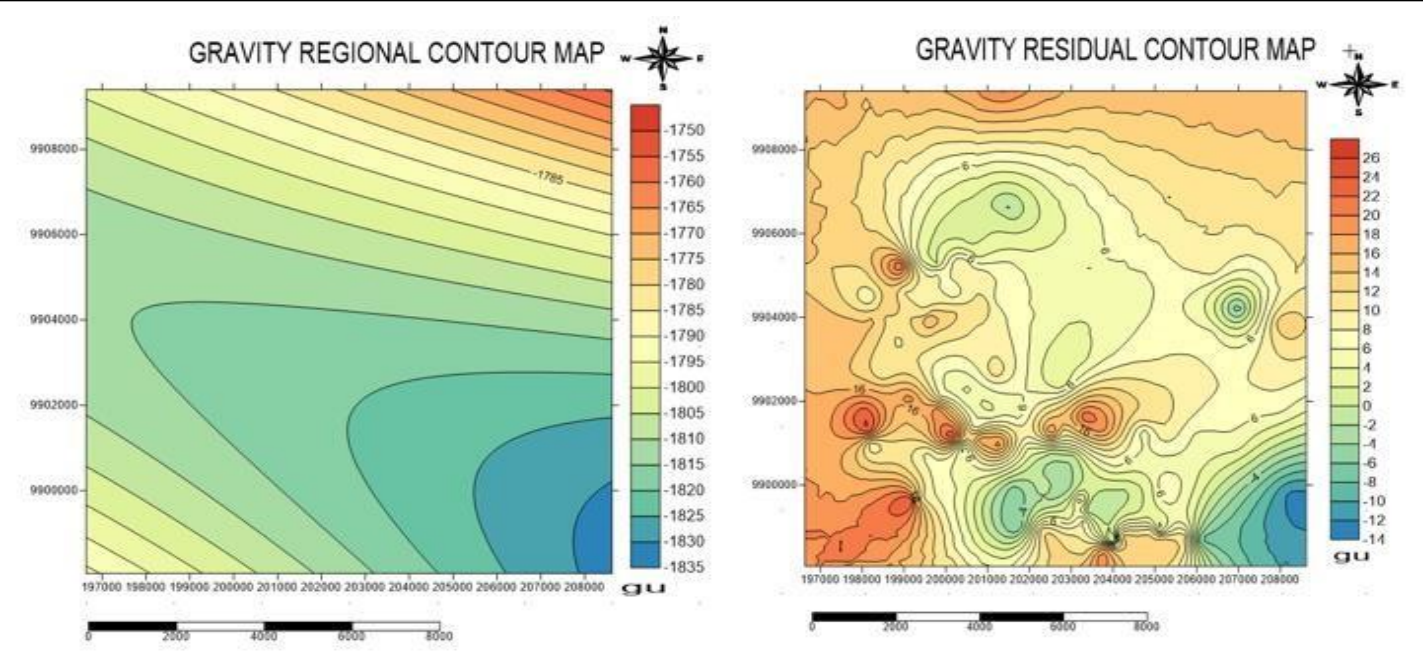


Fig. 3: Gravity regional contour map

Fig. 4: Gravity residual contour map

Lineaments extraction

In order to make better use of this gravity data and to bring out more information compared to those can be drawn from the residual map, lineament extraction techniques were applied to the gravity data to highlight the major structural axis that affect the study area. The lineaments usually appear as straight lines or edges on the anomaly map contributed by lateral variations in gravity anomaly. Knowledge of the user is key in lineaments extraction especially in connecting broken segments into longer segments. Lineaments maps are very useful for localizing the geological contacts because the limit between two blocks of different densities corresponds to this gradient maxim (Aydogan, 2011).

This was done by using the PCI Geomatica's LINE module which is generally utilized to extract linear shapes from the image and produce vector files, using 6 parameters mainly grouped as Edge detection thresholding and curve processes were part of lineament extraction. These parameters defining the discontinuities in the filtered images are complex and depend on the length, the angle and the gradient level thresholds of a pixel or a set of pixels considered as a single linear or curvilinear element (Ahmadi & Pekkan, 2021). The parameters are mainly grouped as follows;

(a) Edge detection

This is enhanced by use of the Gaussian blur which has the best combination of suppression of high frequencies while also minimizing spatial spread. Gaussian blur algorithm Equation 3Equation 1 performs a weighted average operation on the entire image, it is used to reduce image noise by attenuating high frequency signals. Where x is the distance from the origin in the horizontal axis, y is the distance from the origin in the vertical axis, and σ is the standard deviation of the Gaussian distribution (Collins & State, n.d.).

$$G(x, y) = 2 \pi _{1} \sigma e - (x^{2} + y^{2})/2 \sigma 2$$
 Equation 1

(b)Threshold of Edge gradient

Edge Gradient Threshold (GTHR) is minimum value of gradient to be considered as an edge during the edge detection. To compute the image gradients for each pixel x-derivative of Gaussian and y-derivative of Gaussian

32 | Page

filters are used. Then the gradient magnitude and gradient orientation, maps are built based on computed derivatives with respect to x and y for each pixel (Lindeberg, 1998).

(c) Curve extraction

In the third stage, the curves were extracted from the binary edge image depending on the following parameters. Length Threshold (LTHR) which is the minimum length of a curve to be considered as a lineament, Line Fitting Threshold (FTHR) which is the maximum error allowed during the line segment fitting to form a lineament the Angular Difference Threshold (ATHR) which specifies the angle not to be exceeded between two vectors to be linked and the Linking Distance Threshold (DTHR) which is the maximum distance between two vectors to be linked. The extracted curves are then converted to a vector form by fitting line segments to them. The threshold values are shown in table (Farahbakhsh et al., 2020).

Table: Line module parameters used in this study

Parameter	Value
Filter Radius (Pixels)	5
Edge Gradient Threshold	5
Curve Length Threshold (Pixels)	10
Line Fitting Error Threshold (Pixels)	1
Angular Difference Threshold (Degrees)	30
Linking Distance Threshold (Pixels)	10

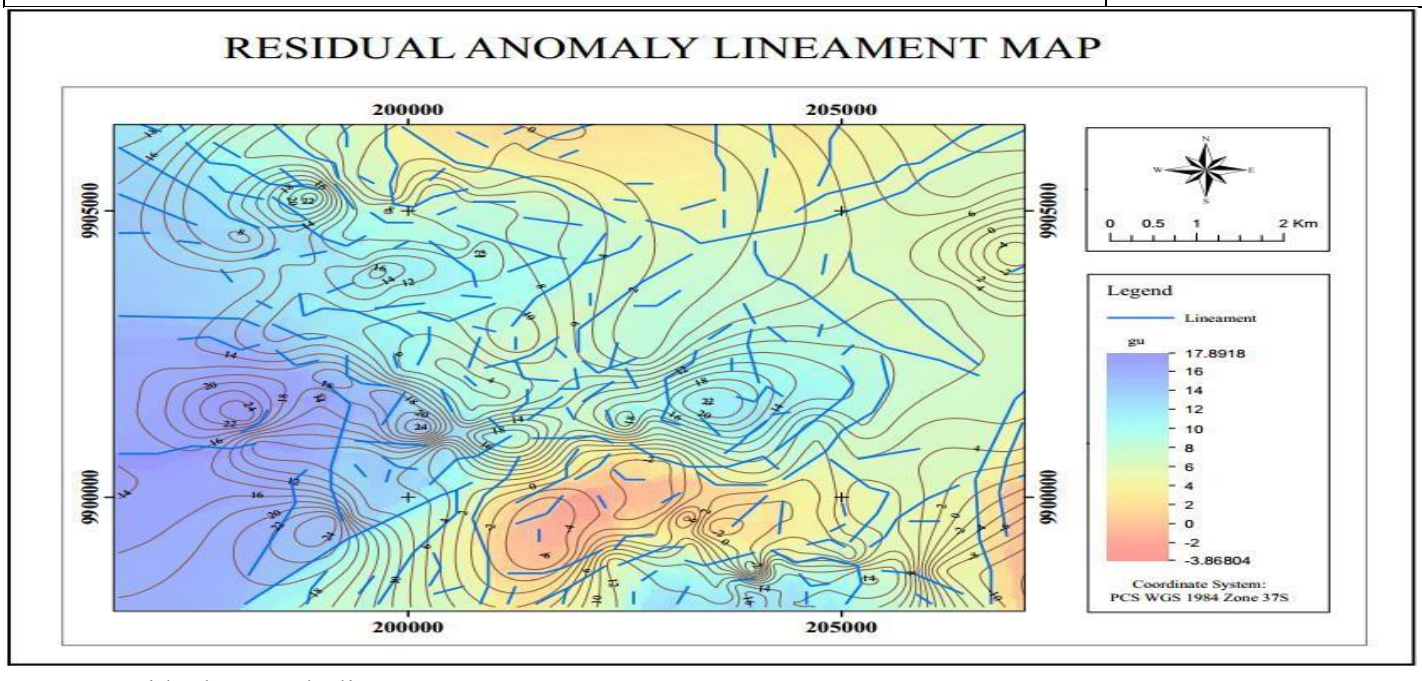


Fig. 5: Residual anomaly lineament map

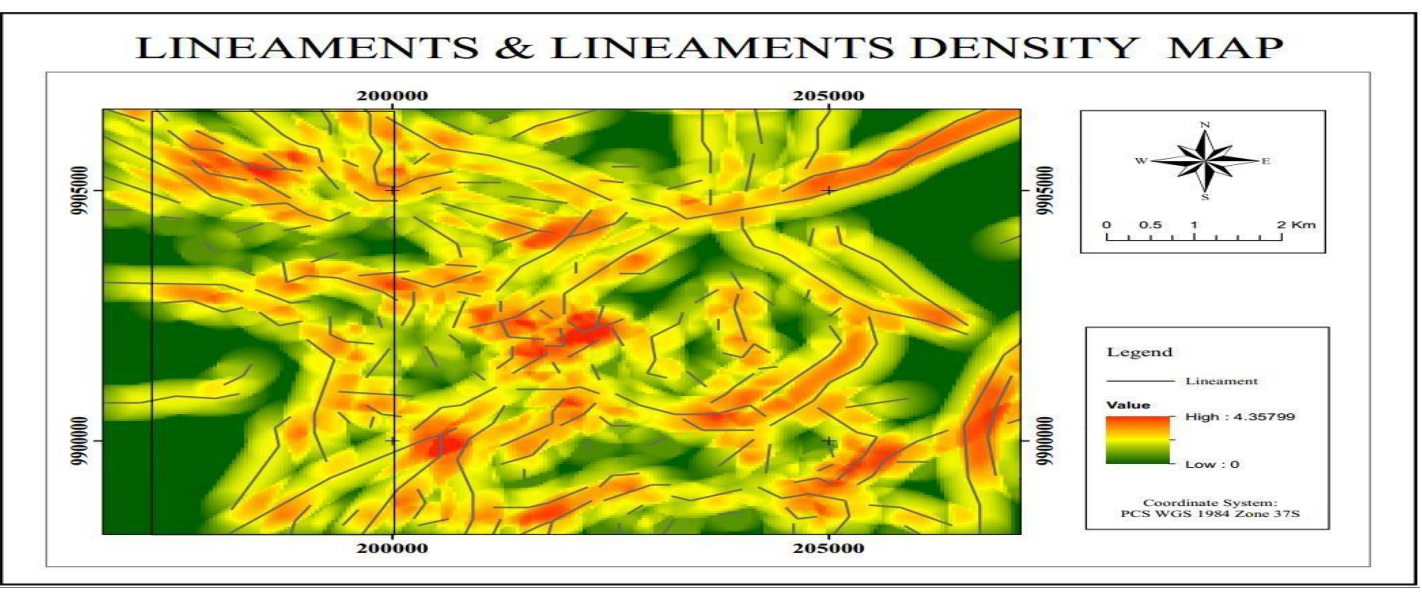


Fig. 6: Density lineament map

III. Discussion

Gravity anomalies are categorized as low medium and high anomaly values. The regional anomaly map represents subsurface conditions of deep structures in Fig. 3, while the residual anomaly map Fig. 5 describe the shallow subsurface information (Nugraha et al., 2021). Residual anomaly map shows that the range of gravity values is about 26gu to -14gu.

Based on the regional anomaly the area cutting across north-western to the south-eastern part of the study area tends to be dominated by high gravity values between -1810gu and – 1835gu. There is a difference between regional and residual anomaly patterns. The western side of the residual map is dominated by low anomalies. The middle zone between the east and the west has structures with high anomalies and the structures with the high anomalies extends towards the east zone. Denser rhyolitic rocks in the central and eastern part causes high anomaly values resulting from existence of volcanic activity in the study area. Pyroclastic rocks as in Fig. 1 that is spread on the western zone of the study area results to low gravity anomalies.

The density analysis calculates the frequency of the lineaments per unit area and then produce a map showing concentrations of the lineaments over unit area. (Sedrette & Rebaï, 2016). Lineaments map and lineaments density map were generated as shown in Fig. 5 and Fig. 6 respectively.

A rose diagram tool was used to derive lineament directions, it corresponds to the directions of the minimum local image gradient and the density of the lineament network. The statistical analysis of the structural lineament layer extracted from the Olkaria geothermal field gravity map reveals that the directions of classes NWSW and E-W are the major directions of the lineament distribution (Fig. 7). The secondary directions are the NESW and N-S classes. Zonation of this field follows faulting lines. The middle fault zone (Fig. 8) lineaments indicate distinctive region of N-S trend which is associated to the faulting between the east and the west zones.

34 | Page

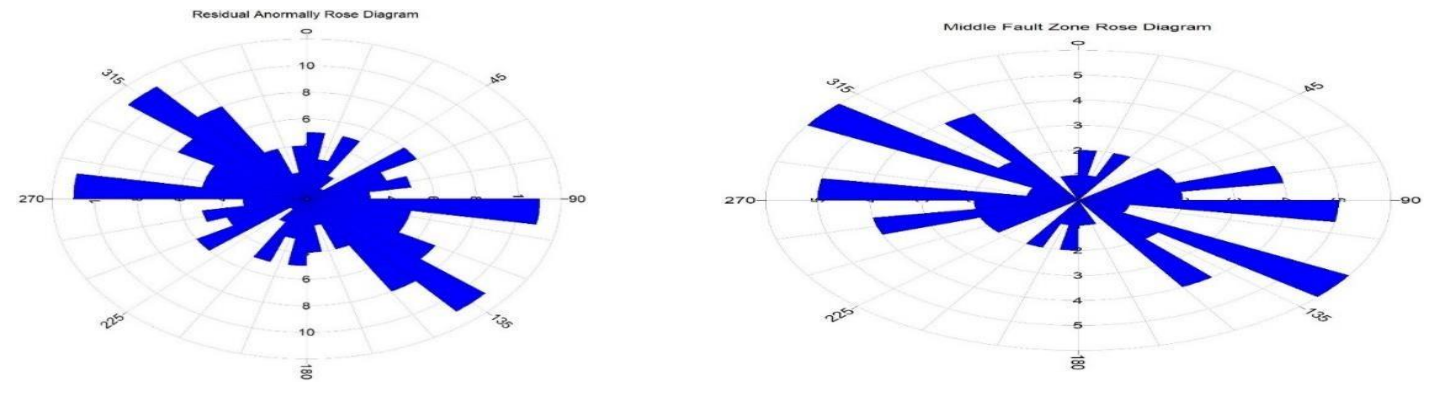


Fig. 7: Entire field Lineaments rose diagram zone

Fig. 8: Middle zone lineaments rose diagram

The young N-S oriented faults represent the most recent tectonic activity on the rift floor, they can be observed from the lineament map and their location in along Ol Njorowa Gorge and Ololbutot fault which is the middle fault zone area between the east and west fields (Mariita et al., 2016). According to Marita, 2016 most of the faults are buried by recent lava flows, their outlines are signaled by fracturing of the lavas in E-W direction due to minimum stress action. Extraction of lineaments from gravity residual map further agrees with study from structural mapping on Olkaria geothermal area by using geochemical soil gas surveys with Munyiri, 2016 where faults were classified under five strikes which are N-S, NE-SW, NW-SE, NNW-SSE and E-W that were formed during different tectonic episodes.

IV. Conclusion

Based on Bouguer residual anomaly map SVD is effective in revealing small, shallow localized structures as viewed from Olkaria geothermal residual contour map. The western zone tends to have less fracturing, also the structures have lower density compared to the eastern zone as observed from the gravity residual contour map. Line module edge enhancement and filtering applied in automatic extraction of lineaments made it easy to overcome visual distinctiveness associated with manual extraction of lineaments in geophysical methods. The lineament density map also reveals low density of lineaments on the western zone.

Rose diagram of the middle fault zone shows the direction of lineaments in NW-SE, N-E and distinctively a N-S trending fault which is subdominant. Faults structures orientations generated by this study compare with orientations of previously mapped structures in Olkaria geothermal field.

References

Ahmadi, H., & Pekkan, E. (2021). Fault-based geological lineaments extraction using remote sensing and GIS—A review. Geosciences (Switzerland), 11(5), 1–32. https://doi.org/10.3390/geosciences11050183

Aydogan, D. (2011). Extraction of lineaments from gravity anomaly maps using the gradient calculation: Application to Central Anatolia. Earth, Planets and Space, 63(8), 903–913. https://doi.org/10.5047/eps.2011.04.003

Darmawan, D., Daud, Y., & Iskandar, C. (2021). Identification of geological structure based on gravity and remote sensing data in "X" geothermal field. AIP Conference Proceedings, 2320. https://doi.org/10.1063/5.0038807

- Farahbakhsh, E., Chandra, R., Olierook, H. K. H., Scalzo, R., Clark, C., Reddy, S. M., & Müller, R. D. (2020). Computer vision-based framework for extracting tectonic lineaments from optical remote sensing data. International Journal of Remote Sensing, 41(5). https://doi.org/10.1080/01431161.2019.1674462
- Geowissenschaften, P. (2015). The role of fault zones on structure, operation and prospects of geothermal reservoirs: A case study in Lahendong, Indonesia.
- Lindeberg, T. (1998). Edge detection and ridge detection with automatic scale selection.
- Mariita, N. O., Training, G. E., Karingithi, C. W., Wanjohi, A. W., Hersir, G., Arnason, K., Steingrimsson, B., Jessica, M. A., Ouma, P., Koech, V., Mwarania, F., Mwangi, S. M., Wamalwa, R. N., Nyamai, C. M., Ambusso, W. J., Mulwa, J., Waswa, A. K., & Munyiri, S. K. (2016). Structural mapping of Olkaria Domes Geothermal Field using geochemical soil gas surveys, remote sensing and GIS. Short Course on Surface Exploration for Geothermal Resources, 7(December).
- Nugraha, G. U., Gaol, K. L., Handayani, L., & Lubis, R. F. (2021). Lineament extraction using gravity data in the Citarum watershed. Indonesian Journal of Geography, 53(1), 87–94. https://doi.org/10.22146/ijg.52402
- Omenda, P. A. (1998). The geology and structural controls of the Olkaria geothermal system, Kenya. Geothermics, 27(1), 55–74. https://doi.org/10.1016/S0375-6505(97)00028-X
- Sedrette, S., & Rebaï, N. (2016). Automatic extraction of lineaments from Landsat ETM+ images and their structural interpretation: Case study in Nefza region (North West of Tunisia). Journal of Research in Environmental and Earth Sciences, August, 139–145. http://earthexplorer.usgs.gov
- Sumintadireja, P., Dahrin, D., & Grandis, H. (2018). A note on the use of the second vertical derivative (SVD) of gravity data with reference to Indonesian cases. Journal of Engineering and Technological Sciences, 50(1), 127–139. https://doi.org/10.5614/j.eng.technol.sci.2018.50.1.9
- Telford, W. M., Geldart, L. P., & Sheriff, R. E. (1990). Applied geophysics (2nd ed.). Cambridge University Press.
- Wamalwa, R. N., Nyamai, C. M., Ambusso, W. J., Mulwa, J., & Waswa, A. K. (2016). Structural controls on the geochemistry and output of the wells in the Olkaria Geothermal Field of the Kenyan Rift Valley. International Journal of Geosciences, 7(11), 1299–1309. https://doi.org/10.4236/ijg.2016.711094